The natural history of Leber congenital amaurosis and cone-rod dystrophy associated with variants in the GUCY2D gene

Hahn, L.C.; Georgiou, M.; Almushattat, H.; Schooneveld, M.J. van; Carvalho, E.R. de; Wesseling, N.L.; ... ; Boon, C.J.F.

AMERICAN ACADEMY OF OPHTHALMOLOGY®

The Natural History of Leber Congenital Amaurosis and Cone–Rod Dystrophy Associated with Variants in the *GUCY2D* Gene

Leo C. Hahn, MD,[1] Michalis Georgiou, MD, PhD,[2] Hind Almushattat, BSc,[1] Mary J. van Schooneveld, MD, PhD,[1,3] Emanuel R. de Carvalho, MD, PhD,[2] Nieneke L. Wesseling, MD,[1] Jacoline B. ten Brink, BAS,[4] Ralph J. Florijn, PhD,[4] Birgit I. Lissenberg-Witte, PhD,[5] Ine Strubbe, MD,[6] Caroline van Cauwenbergh, PhD,[6,7] Julie de Zaeytijd, MD,[6] Sophie Walraedt, MD,[6] Elfride de Baere, MD, PhD,[6,7] Rajarshi Mukherjee, MD,[8] Martin McKibbin, MD,[8] Magda A. Meester-Smoor, PhD,[9] Alberta A.H.J. Thiadens, MD, PhD,[9] Saoud Al-Khuzaei, MD,[10] Engin Akyol, MD,[11] Andrew J. Lotery, MD,[11] Maria M. van Genderen, MD, PhD,[3,12] Jeannette Ossewaarde-van Norel, MD, PhD,[12] L. Ingeborgh van den Born, MD, PhD,[13] Carel B. Hoyng, MD, PhD,[14] Caroline C.W. Klaver, MD, PhD,[9,14] Susan M. Downes, MBChB, MD(R),[10] Arthur A. Bergen, PhD,[4,15] Bart P. Leroy, MD, PhD,[6,7,16] Michel Michaelides, MD(Res), FRCOphth,[2,17] Camiel J.F. Boon, MD, PhD[1,18]

Objective: To describe the spectrum of Leber congenital amaurosis (LCA) and cone–rod dystrophy (CORD) associated with the *GUCY2D* gene and to identify potential end points and optimal patient selection for future therapeutic trials.

Design: International, multicenter, retrospective cohort study.

Subjects: Eighty-two patients with *GUCY2D*-associated LCA or CORD from 54 families.

Methods: Medical records were reviewed for medical history, best-corrected visual acuity (BCVA), ophthalmoscopy, visual fields, full-field electroretinography, and retinal imaging (fundus photography, spectral-domain OCT [SD-OCT], fundus autofluorescence).

Main Outcomes Measures: Age of onset, evolution of BCVA, genotype–phenotype correlations, anatomic characteristics on funduscopy, and multimodal imaging.

Results: Fourteen patients with autosomal recessive LCA and 68 with autosomal dominant CORD were included. The median follow-up times were 5.2 years (interquartile range [IQR] 2.6–8.8 years) for LCA and 7.2 years (IQR 2.2–14.2 years) for CORD. Generally, LCA presented in the first year of life. The BCVA in patients with LCA ranged from no light perception to 1.00 logarithm of the minimum angle of resolution (logMAR) and remained relatively stable during follow-up. Imaging for LCA was limited but showed little to no structural degeneration. In patients with CORD, progressive vision loss started around the second decade of life. The BCVA declined annually by 0.022 logMAR ($P < 0.001$) with no difference between patients with the c.2513G>A and the c.2512C>T *GUCY2D* variants ($P = 0.798$). At the age of 40 years, the probability of being blind or severely visually impaired was 32%. The integrity of the ellipsoid zone (EZ) and that of the external limiting membrane (ELM) on SD-OCT correlated significantly with BCVA (Spearman $\rho = 0.744$, $P = 0.001$, and $\rho = 0.712$, $P < 0.001$, respectively) in those with CORD.

Conclusions: Leber congenital amaurosis associated with *GUCY2D* caused severe congenital visual impairment with relatively intact macular anatomy on funduscopy and available imaging, suggesting long preservation of photoreceptors. Despite large variability, *GUCY2D*-associated CORD generally presented during adolescence, with a progressive loss of vision, and culminated in severe visual impairment during mid-to-late adulthood. The integrity of the ELM and EZ may be suitable structural end points for therapeutic studies of *GUCY2D*-associated CORD. *Ophthalmology Retina 2022;6:711-722 © 2022 by the American Academy of Ophthalmology. This is an open access article under the CC BY-NC-ND license (http://creativecommons.org/licenses/by-nc-nd/4.0/).*

Supplemental material available at www.ophthalmologyretina.org.

Leber congenital amaurosis (LCA) and cone–rod dystrophy (CORD) are relatively common inherited retinal dystrophies (IRDs) that frequently lead to significant visual impairments in young patients.[1–3] Typically, LCA causes severe congenital visual impairment or blindness with absent-to-minimal residual electroretinography (ERG) responses, often in combination with nystagmus, photophobia, and eye poking.[2,4] Patients with CORD tend to present with mild-to-

https://doi.org/10.1016/j.oret.2022.03.008
ISSN 2468-6530/22

moderate loss of visual acuity and/or color vision disturbance within the first decades of life, which generally progresses to severe visual impairment or even legal blindness during adulthood.[5,6] One of the most common genes causing these conditions is the *GUCY2D* gene, which has been found to be responsible for up to 20% of all LCA and up to 25% of all autosomal dominant CORD cases.[3,4]

The *GUCY2D* gene encodes the enzyme retinal guanylate cyclase 1, which plays a crucial role in photoreceptors' recovery to the dark-adapted state by regulating intracellular calcium concentration.[7] Currently, there is no treatment available for patients with IRDs associated with *GUCY2D*; however, for *GUCY2D*-associated LCA, improvements in electrophysiology and visual function were seen after experimental gene replacement therapy in animal and preliminary human phase I/II studies.[8,9]

Interestingly, the great majority of patients with CORD associated with *GUCY2D* have disease-causing variants in codon 838, out of which up to 87% are the 2 most prevalent variants described in the current study.[10] The high prevalence of these variants and their proximity to each other make them attractive potential targets for gene-editing approaches. In animal models, CRISPR/Cas9 was successfully used to knock out *GUCY2D* expression, which may be a viable first step toward a therapeutic approach for *GUCY2D*-associated CORD.[11]

To select the most appropriate design for human gene therapy trials as well as the most suitable candidates and clinical end points for such trials, a thorough understanding of the IRDs associated with *GUCY2D* is essential. In addition, patients and clinicians will benefit from such insights to enable more accurate clinical and prognostic information. Therefore, this international, multicenter, retrospective study aimed to deliver a detailed description of the natural courses, phenotypes, and genotypes of *GUCY2D*-associated LCA and CORD.

Methods

Study Population and Data Collection

Patient data were collected from the Delleman archive, a large database for inherited eye diseases at the Amsterdam University Medical Centers (Amsterdam, The Netherlands), and various Dutch expertise centers within the RD5000 consortium, a national consortium for IRDs.[12] Additional patients were included from the University Hospital Ghent (Ghent, Belgium) as well as from 4 academic tertiary referral centers in the United Kingdom (Moorfields Eye Hospital, St James's University Hospital Leeds, Oxford Eye Hospital, and University Hospital Southampton). For inclusion, patients needed either a molecularly confirmed diagnosis or a typical clinical presentation and an affected first-degree family member with a confirmed disease-causing *GUCY2D* variant. This study was approved by the ethics committee of the Erasmus Medical Center and adhered to the tenets of the Declaration of Helsinki. Informed consent was obtained from patients or their legal guardians. For patients of the University Hospital Ghent the need for informed consent was waived by the local ethics committee since only pseudonymized data was used. Eighteen patients with CORD from 4 families have been described previously, but substantial new follow-up data are described in this article.[13–15] Additionally, for 13 of these patients from a large Dutch family, the *GUCY2D* gene had not been identified as the disease-causing gene in the previous publication from 1992.[15]

Data collection was performed through the standardized review of medical records for medical history, age at onset, symptoms, family history, best-corrected visual acuity (BCVA), refractive error, dilated fundus examination, full-field ERG, Goldmann visual field testing, color vision testing, spectral-domain OCT (SD-OCT), fundus autofluorescence (FAF) images, and color fundus photography. Measurements of retinal thickness and the evaluation of layer integrity on SD-OCT were performed within a radius of 500 μm around the foveal center in the Heidelberg Eye Explorer (Heidelberg Engineering). The integrity of the ellipsoid zone (EZ) and the external limiting membrane (ELM) were graded as either intact, disrupted, or absent by 2 independent graders (L.C.H. and H.A.). The graders were also masked for other image modalities. Weighted Cohen κ analyses were performed and showed high interrater reliability for the integrity of EZ ($\kappa = 0.892 \pm 0.03$; $P < 0.001$) as well as for ELM integrity ($\kappa = 0.918 \pm 0.02$; $P < 0.001$). For the 12 cases in which the graders disagreed, a trained expert referee (C.J.F.B.) decided on the subgroup. The autofluorescence patterns on FAF images were described for each patient by a retinal specialist (C.J.F.B.), and the frequencies for each pattern were subsequently reported.

Statistical Analysis

For statistical analysis, SPSS version 23.0 (IBM Corp) and the R software environment were used.[16] Categorical data were expressed as proportions. Continuous data were reported as either means with standard deviations or medians with interquartile ranges (IQRs). A multistate model was used to estimate the disease progression based on categories of visual impairment with the R-package msm. The following states were used, as defined by the World Health Organization, based on the better-seeing eye: mild visual impairment ($20/67 \leq$ BCVA $< 20/40$), moderate visual impairment ($20/200 \leq$ BCVA $< 20/67$), severe visual impairment ($20/400 \leq$ BCVA $< 20/200$), and blindness (BCVA $< 20/400$).[17] Linear mixed models were applied to analyze the annual rate of decline of BCVA using data from both eyes. To account for intereye correlation, a random intercept was added to the model.[18] For this analysis, the BCVA values were converted to logarithm of the minimum angle of resolution (logMAR). For hand movement, a value of 2.7 logMAR was used; for light perception, 2.8; and for no light perception, 2.9. Asymmetry of BCVA was defined as a minimum difference of 0.3 logMAR between the right and left eye at 2 consecutive visits.[19]

Results

Participants

In total, 82 patients from 54 families were included in this study. Fourteen (17.1%) were diagnosed with autosomal recessive LCA, and 68 (82.9%) were diagnosed with autosomal dominant CORD. For 65 out of 82 (79.3%) patients, follow-up data were available, with a median follow-up time of 7.0 years (IQR 2.7−14.2 years) and a mean number of visits of 3.0 (IQR 2.0−6.5). The clinical characteristics of the cohort are presented by group in Table 1.

Disease Onset, Reported Symptoms, and Visual Acuity

The median age at onset of LCA was 0.3 years, with a range of 0.0 to 2.2 years, and patients presented with congenital severe

Table 1. Clinical Characteristics of Patients with *GUCY2D*-Associated LCA and CORD

Characteristic	LCA (n = 14)	CORD (n = 68)
Gender		
Male, n (%)	6/14 (43)	32/68 (47)
Female, n (%)	8/14 (57)	36/68 (53)
Age at onset, n (%)*	14/14 (100)	49/68 (72)
Median (IQR), yrs	0.3 (0.0–0.6)	14.7 (10.0–26.5)
Range, yrs	0.0–2.2	2.0–40.0
Age at last examination		
Mean ± SD, yrs	13.2 ± 11.3	42.5 ± 16.3
Median (IQR), yrs	9.9 (7.1–16.4)	40.5 (32.1–54.0)
Range, yrs	0.6–35.6	9.9–78.4
Number of visits		
Mean ± SD	4.2 ± 2.0	5.3 ± 4.0
Median (IQR)	3.0 (3.0–5.0)	4.0 (3.0–7.0)
Range	2.0–8.0	2.0–21.0
Follow-up time, n (%)*	12/14 (86)	53/68 (78)
Median follow-up time (IQR), yrs	5.2 (2.6–8.8)	7.2 (2.2–14.2)
Range, yrs	0.2–15.9	0.3–77.7
Spherical equivalent refraction, n (%)*	6/14 (43)	35/68 (52)
Median (IQR), D	2.3 (2.0 to 4.9)	−4.1 (−6.6 to −0.6)
Range, D	1.4 to 9.0	−18.8 to 2.6
High myopia (< −6), n (%)	0/13 (0)	10/35 (29)
Moderate myopia (−3 D > SER ≥ −6 D), n (%)	0/13 (0)	8/35 (23)
Mild myopia (−0.75 D > SER ≥ −3 D), n (%)	0/13 (0)	6/35 (17)
SER ≥ −0.75, n (%)	6/6 (100)	11/35 (31)
Last available BCVA better-seeing eye, n (%)*	12/14 (86)	67/68 (99)
Median BCVA, logMAR (IQR)	2.8 (1.4–2.8)	0.9 (0.26–1.3)
Median BCVA, Snellen equivalent (IQR)	LP (LP to 20/500)	20/150 (20/400–20/36)
Last available BCVA worse-seeing eye, n (%)*	12/14 (86)	67/68 (99)
Median BCVA, logMAR (IQR)	2.8 (2.6–2.8)	1.0 (0.5–1.6)
Median BCVA, Snellen equivalent (IQR)	LP (LP to CF)	20/200 (20/660–20/67)
Recorded symptoms†, n (%)*	14/14 (100)	65/68 (96)
Nystagmus	11/14 (79)	0/65 (0)
Photophobia	6/14 (43)	24/65 (37)
Nyctalopia	1/14 (7)	1/65 (2)
Color vision disturbance	1/14 (7)	14/65 (22)
Full-field electroretinogram pattern, n (%)*	5/14 (36)	35/68 (52)
Scotopic and photopic extinguished	5/5 (100)	0/35 (0)
Cone isolated	0/5 (0)	17/35 (49)
Cone–rod pattern	0/5 (0)	14/35 (40)
Normal	0/5 (0)	4/35 (11)

BCVA = best-corrected visual acuity; CF = counting fingers; CORD = cone–rod dystrophy; D = diopters; IQR = interquartile range; LCA = Leber congenital amaurosis; logMAR = logarithm of the minimum angle of resolution; LP = light perception; SD = standard deviation; SER = spherical equivalent refraction.
*Availability of data.
†Patients could present multiple different symptoms simultaneously.

visual impairment. Nystagmus was reported in 11 of 14 (78.6%) patients, photophobia in 6 of 14 (42.9%), eye poking in 5 of 14 (35.7%), and nyctalopia in 1 of 14 (7.1%). Visual acuity data were available for 12 of 14 (85.7%) patients and ranged from no light perception to 1.0 logMAR (20/200 Snellen equivalent). The visual acuity did not change significantly during the follow-up ($P = 0.811$).

In patients with CORD, the reported median age at onset was 14.6 years (IQR 10.0–26.5 years). Patients presented with either mild central vision loss, color vision disturbances, or both simultaneously (Table 1). In one Dutch family, extensive color vision testing in 3 young asymptomatic family members revealed a tritan color vision disturbance as the first symptom, and the loss of visual acuity only started to develop at later ages. The BCVA declined at a rate of 0.022 logMAR annually in patients with CORD ($P < 0.001$) based on data of both eyes (Fig 1). The probabilities of being in different states of visual impairment based on the better-seeing eye, by age, are illustrated in Figure 1 and Table S1 (available at www.ophthalmologyretina.org). The BCVA between eyes was strongly correlated (Spearman $\rho = 0.897$, $P < 0.001$). Asymmetry in BCVA between eyes was seen in 1 of 14 (7.1%) patients with LCA and in 13 of 67 (19.4%) patients with CORD.

Ophthalmic Findings, Funduscopy, and Multimodal Imaging

In 3 of 14 (21.4%) patients with LCA, an abnormal foveal reflex was described in funduscopic reports. Two (14.3%) patients with LCA were reported to have peripheral mottled retinal pigment

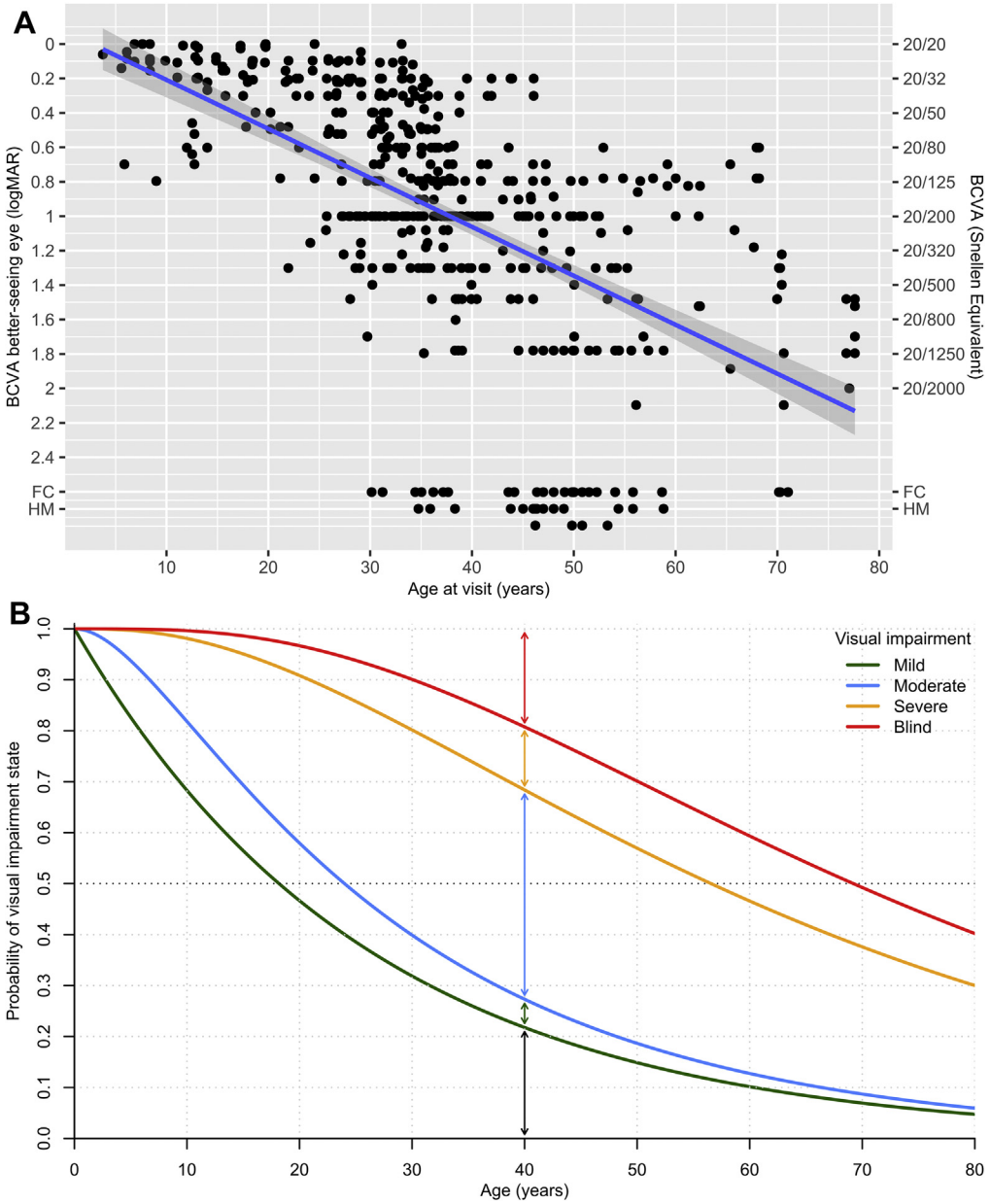

Figure 1. Evolution of visual acuity in autosomal dominant CORD associated with *GUCY2D*. **A,** Plot of the linear mixed model using the cross-sectional and longitudinal BCVA measurements of both eyes to predict the average evolution of BCVA with increasing age. In the entire population of patients with *GUCY2D*-associated CORD, a significant annual decline of 0.022 logMAR ($P < 0.001$) was found. **B**, Graph displaying the disease progression estimated by a multistate model in the better-seeing eye. The curves represent the probabilities of having mild visual impairment (20/67 ≤ BCVA < 20/40), moderate visual impairment (20/200 ≤ BCVA < 20/67), severe visual impairment (20/400 ≤ BCVA < 20/200), and blindness (BCVA < 20/400). The distances between the curves indicate the probability of being in a certain category of visual impairment at each age. The distance between the 0% mark and the green line represents the probability of having no significant visual impairment; the distance between the green and blue lines represents the probability of having mild visual impairment; the distance between the blue and yellow lines represents the probability of having moderate visual impairment; the distance between the yellow and red lines represents severe visual impairment; and the distance between the red line and 100% mark represents the probability of being blind for each age. At an age of 40 years, the multistate model estimated that patients with *GUCY2D*-associated CORD have a probability of 21.8% to have no significant visual impairment, 5.5% to have mild visual impairment, 41.1% to have moderate visual impairment, 12.4% to have severe visual impairment, and 19.2% to be blind (further specification of all probabilities at different ages can be found in Table S1, available at www.ophthalmologyretina.org). BCVA = best-corrected visual acuity; CORD = cone–rod dystrophy; FC = finger counting; HM = hand movements; logMAR = logarithm of the minimum angle of resolution.

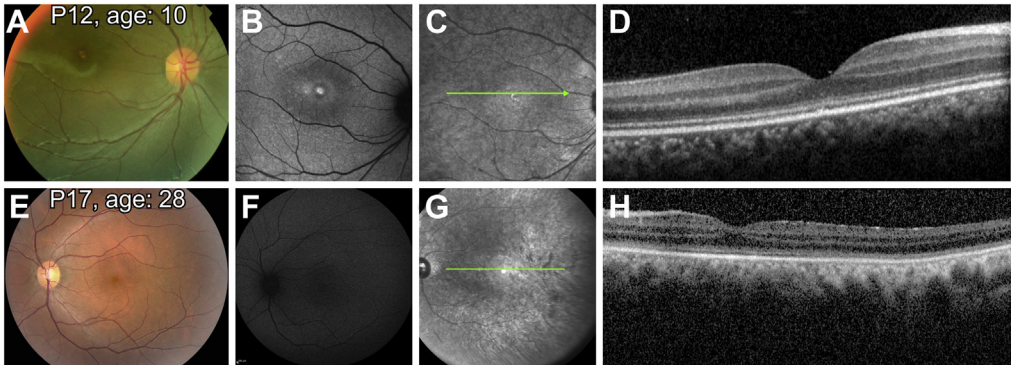

Figure 2. Findings on imaging of 2 patients with *GUCY2D*-associated Leber congenital amaurosis. **A–D,** Fundus photograph (**A**), a fundus autofluorescence image (**B**), a near-infrared image (**C**), and an SD-OCT scan (**D**) of a 10-year-old patient with heterozygous missense variants in *GUCY2D* (c.2620G>A; p.(Glu874Lys) and c.2939A>C; p.(His980Pro)). On color fundus photography (**A**), mild foveal retinal pigment epithelium alterations were seen, and on SD-OCT (**D**), intact retinal anatomy was seen. On fundus autofluorescence (**B**), hyperautofluorescent changes in the fovea were seen, surrounded by a slightly hypoautofluorescent ring with hyperautofluorescent borders. The BCVA was 20/400 in both eyes. **E–H,** A fundus photograph (**E**), a fundus autofluorescence image (**F**), a near-infrared image (**G**), and an SD-OCT scan (**H**) of a 28-year-old patient (homozygous c.1694T>C; p.(Phe565Ser) *GUCY2D* variants) with nearly normal appearance on imaging. The BCVA was light perception in both eyes. BCVA = best-corrected visual acuity; SD-OCT = spectral-domain OCT.

epithelium (RPE) pigmentation, and 1 of 14 (7.1%) patients had RPE atrophy in the peripheral retina. Bilateral optic disc pallor was found in 1 of 14 (7.1%) patients. Spectral-domain OCT and FAF imaging were available for 8 of 14 (57.1%) subjects with LCA, but the imaging quality was variable because of nystagmus and only 3 of 14 (21.4%) had macular scans of sufficient quality. These 3 SD-OCT scans showed remarkably intact retinal structures and photoreceptor layers in the peripheral and central retinas (Fig 2). On FAF imaging, in 3 of 8 (37.5%) patients with LCA, central autofluorescence was slightly increased, resulting in a lack of normal foveal hypoautofluorescence (Fig 2F). Three patients with LCA (21.4%) had complications likely caused by eye poking, including bilateral keratoconus, disrupted Descemet membranes, hydrops, leucoma, corneal scars, and cortical cataract. The cortical cataract developed at the age of 6 in the right eye, and the patient underwent uncomplicated cataract surgery with intraocular lens insertion 1 year later. The BCVA before and after surgery was light perception.

The most prominent funduscopic findings described in patients with CORD included macular RPE atrophy in 16 of 65 (24.6%) patients, macular RPE alteration in 18 of 65 (27.7%), macular mottling in 20 of 65 (30.8%), and bull's-eye maculopathy in 6 of 65 (9.2%) based on the descriptions in the case notes. In the peripheral retina, RPE atrophy was reported in 1 of 65 patients (1.5%), RPE alterations in 4 of 65 patients (6.2%), and latticelike lesions in 1 of 65 patients (1.5%). Attenuated retinal blood vessels were recorded in 10 of 65 (15.4%) and cataracts in 8 of 65 (12.3%) patients with CORD. Myopia was found in 24 of 35 (68.6%) patients, and high myopia (>−6 diopters) was found in 10 of 35 (28.5%) patients. Patients with high myopia did not show more severe annual decreases in BCVA than the rest of the cohort ($P = 0.738$).

Spectral-domain OCT scans were available for 46 of 68 (67.6%) and FAF images for 45 of 68 (66.2%) patients with CORD. The imaging showed increased central autofluorescence in the early stages, which progressed toward macular atrophy and central absence of autofluorescence (Fig 3). All patients had FAF abnormalities. The frequency of FAF patterns found in this cohort together with the integrity of EZ and ELM on SD-OCT are displayed in Table 2. One patient had drusenoid, hyperautofluorescent dots on FAF (Fig 4D–H). The disruption and the absence of the foveal EZ and ELM layer correlated strongly with a decrease in BCVA (Spearman $\rho = 0.744$, $P < 0.001$, and $\rho = 0.712$, $P < 0.001$, respectively). The median central retinal thickness (CRT) was 142.0 μm (IQR 119.5–189.0 μm) and decreased by 2.7 μm ($P < 0.001$) annually. The CRT correlated strongly between eyes (Spearman $\rho = 0.933$, $P < 0.001$) but only showed a moderate negative correlation with BCVA (Spearman $\rho = -0.551$. $P < 0.001$). Correlation plots regarding the CRT and integrity of the EZ and ELM are displayed in Figure S1 (available at www.ophthalmologyretina.org). In 8 of 46 patients (17.4%), a hyporeflective space (optical gap) beneath the macula was seen on SD-OCT at a median age of 49.0 years (range 21.2–68.0 years; Fig 3D).

FullField ERG and Visual Fields

Electroretinography findings were recorded for 5 of 14 (35.7%) patients with LCA at a median age of 1.4 years (range 0.2–1.8 years); all had fully extinguished scotopic and photopic responses (Table 1).

Full-field ERG examination data were available for 35 of 68 (51.5%) patients with CORD. Most commonly, isolated cone dysfunctions were seen in 17 of 35 (48.6%) patients at a median age of 33.3 years (IQR 30.3–38.3 years), and cone–rod patterns were seen in 14 of 35 (40.0%) patients at a median age of 35.7 years (IQR 30.2–46.9 years). Four (11.4%) patients had normal ERGs at a median age of 19 years (range 5–34 years). Goldmann visual fields were available for 12 of 68 (16.6%) patients with CORD. In 9 of 12 patients (75.0%), the Goldmann visual field showed central scotomas; in 2 of 12 (16.6%), ring scotomas; and in 1 of 12 (8.3%) patients, no visual field defects.

Genetic Characteristics and Genotype–Phenotype Correlations

In the patients with LCA, a total of 14 different *GUCY2D* variants were identified. Ten (71.4%) of these variants were missense

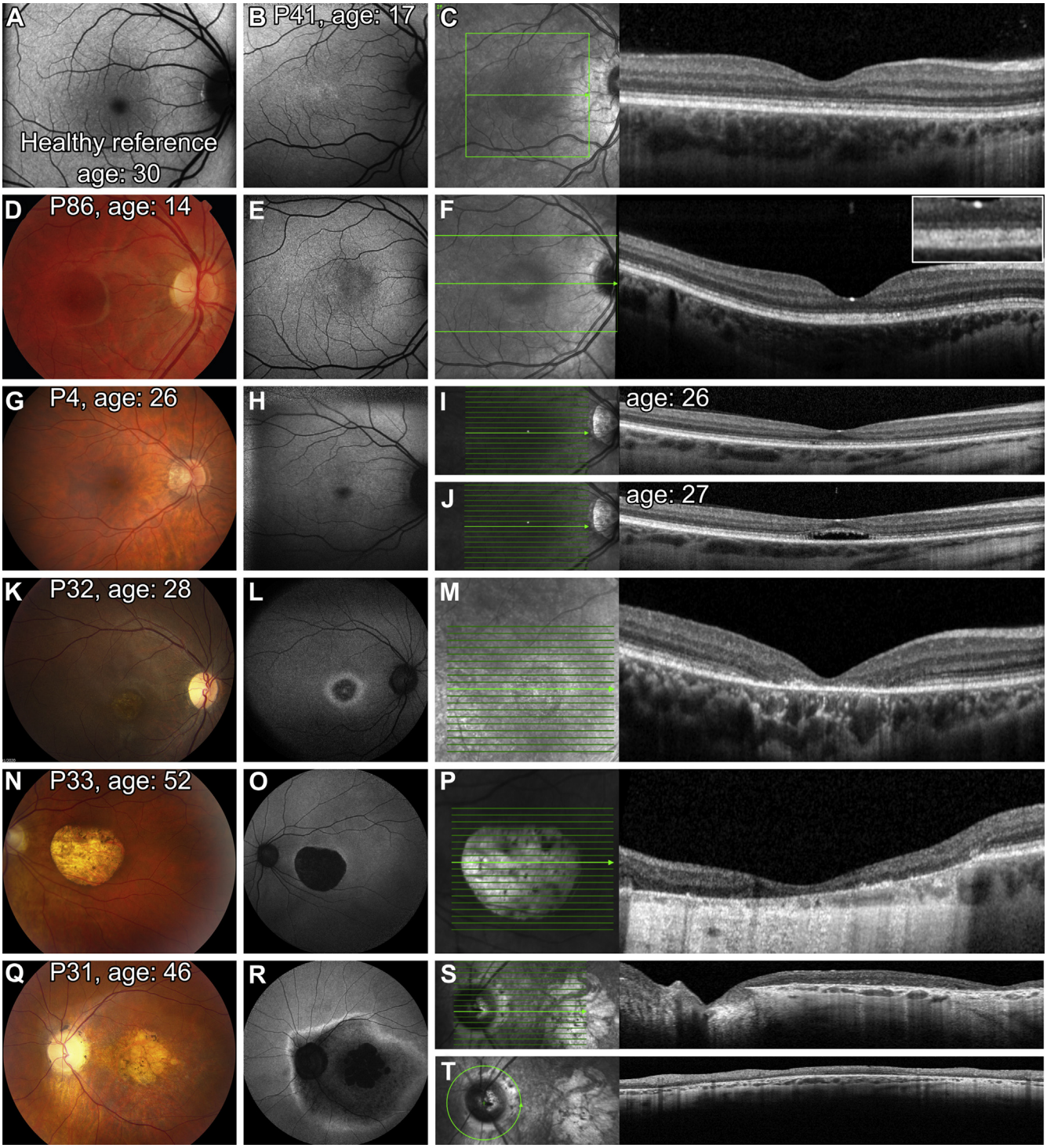

Figure 3. Spectrum of findings on imaging in patients with *GUCY2D*-associated CORD. **A,** Normal fundus autofluorescence image of a 30-year-old healthy male, as a reference, showing typical central hypoautofluorescence in the macular area. **B, C,** Fundus autofluorescence image (**B**) and SD-OCT scan (**C**) of a 17-year-old-patient (c.2513C>T; p.(Arg838Cys) variant in *GUCY2D*). On fundus autofluorescence (**B**), an absence of normal central hypoautofluorescence can be seen compared with the healthy reference (**A**). Spectral-domain OCT (**C**) showed a continuous ELM and EZ, with possibly mild irregularity of the subfoveal EZ. The visual acuity was 20/33 in the right eye and 20/32 in the left eye. **D—F,** A fundus photograph (**D**), a fundus autofluorescence image (**E**), and an SD-OCT scan (**F**) of the left eye of a 14-year-old patient (c.2513C>T; p.(Arg838Cys) variant in *GUCY2D*). The fundus photograph was normal, but an absence of foveal hypoautofluorescence was observed (**E**). On the SD-OCT scan (**F**), the central EZ layer seemed slightly thickened. The visual acuity was 20/80 in both eyes. **G—J,** A fundus photograph (**G**), a fundus autofluorescence image (**H**), and SD-OCT scans (**I, J**) of the left eye of a 26-year-old patient (c.2513C>T; p.(Arg838Cys) variant in *GUCY2D*) with a relatively normal presentation on the color fundus photograph (**G**) and fundus autofluorescence image (**H**). On SD-OCT (**I**), at the age of 26, slight focal disruption of the EZ was present, with an ELM in the macular

mutations, 3 (31.4%) were nonsense mutations, and 1 (7.1%) was a frameshift mutation (Tables S2 and S3, available at www.ophthalmologyretina.org). Two of the patients with LCA (patients 27 and 28) were siblings, whereas the remaining 12 patients were isolated cases. The most common variant in these patients was c.1694T>C (p.(Phe565Ser)), which was found in 4 patients, with 3 being homozygous and 1 being compound heterozygous. Four patients were compound heterozygous for c.2302C>T (p.(Arg768Trp)), with different variants on the other allele. The 2 siblings mentioned before both had a homozygous c.2773G>T (p.(Glu925*)) variant that has not been reported before. Other novel variants in this cohort were the c.518dup (p.(Tyr173*)), c.2861_2862del (p.(Leu954fs*16)), and c.2939A>C (p.(His980Pro)) variants. The c.2620G>A (p.(Glu874Lys)) variant found in patient 12 was reported earlier in a case of autosomal recessive CORD, but to our knowledge, it has not been reported in LCA yet.[20]

In those with CORD, 3 different variants were found, all of which involved codon 838 (Tables S3 and S4, available at www.ophthalmologyretina.org). The most common variant was c.2513G>A (p.(Arg838His)), which was found in 37 of 68 (54.4%) patients from 16 different families. This included 1 large, multigenerational family of 15 affected members from The Netherlands. The c.2512C>T (p.(Arg838Cys)) variant was present in 30 of 68 (44.1%) patients from 24 families. The aforementioned variants were both missense variants. One patient with CORD (1.5%) had the complex (p.(Glu837_Arg838delinsAspSer)) variant and had an atypical phenotype with extensive atrophy in the entire inferior pole (Fig 4A–C). The BCVA at baseline and the rate of BCVA decline did not differ between patients with the c.2513G>A and the c.2512C>T variants ($P = 0.625$ and $P = 0.748$, respectively; Fig S2, available at www.ophthalmologyretina.org).

Discussion

This large, multicenter, retrospective cohort study describes the spectrum of phenotypes, genotypes, and natural courses of 14 patients with autosomal recessive LCA and 68 patients with autosomal dominant CORD from 54 presumably unrelated families with disease-causing variants in the *GUCY2D* gene.

The patients with LCA in this cohort showed severe congenital visual impairment, often in combination with nystagmus and photophobia. This presentation has also been observed in LCA associated with other genes[2]; however, in contrast to many other LCA-associated genes, the visual acuity, albeit often severely reduced, seemed to remain relatively stable during the follow-up in this cohort of patients with *GUCY2D*-associated LCA, and only subtle retinal changes were reported on funduscopy. In the 3 patients with LCA with SD-OCT imaging of sufficient quality, relatively intact retinal structures were observed. This is in accordance with earlier studies on *GUCY2D*-associated LCA, in which slight deterioration of visual acuity and retinal structure was mostly described in patients above 47 years of age[4]; however, other studies have shown the possible slow decrease of foveal outer nuclear layer thickness and decrease of EZ reflectivity in younger patients with *GUCY2D*-associated LCA.[21,22] The description of patients of older age and with longer follow-up periods in future studies may be informative to better determine the long-term functional and structural natural courses of LCA associated with *GUCY2D*.

The study by Bouzia et al[4] also found 6 relatively milder LCA cases, with 2 patients even having a visual acuity of 20/60. This was hypothesized to be due to the presence of at least 1 missense variant in *GUCY2D* exon 2, which presumably causes a less severe phenotype.[4] In our study, on the contrary, visual acuity ranged from no light perception to only 20/200, and the only included patient with a missense variant in exon 2 (c.587A>T (p.(Glu196Val)) had a BCVA of 20/400 at the age of 24 years.

In the patients with CORD in this cohort, disease onset occurred in the second decade of life and showed a gradual decline in visual acuity of 0.022 logMAR per year. At 56 years, there was a 50% estimated probability of having severe visual impairment or being blind based on the better-seeing eye. Funduscopic reports and imaging in those with CORD showed the progressive development of macular atrophy with increasing age, which can also involve the peripapillary area. The majority of patients with *GUCY2D*-associated CORD were myopic; some had severe myopia, which is in accordance with earlier studies.[5,6,10]

Eight patients with CORD had a hyporeflective space (optical gap) beneath the macula on SD-OCT (Fig 3J), mimicking subretinal fluid; however, this phenomenon has been described previously in IRDs and is hypothesized to represent not the primary leakage of fluid but, rather, an empty space as a result of outer photoreceptor tissue loss.[23]

area that was largely intact and a BCVA of 20/50. Interestingly, 1 year later, this patient developed bilateral, hyporeflective spaces (optical gap) in the central maculae, mimicking subretinal fluid accumulation (**J**). The BCVA dropped to 20/100 in the left eye at this last visit. **K–M,** A color fundus photograph (**K**), a fundus autofluorescence image (**L**), and an SD-OCT image (**M**) of a 28-year-old patient (c.2512C>T; p.(Arg838Cys) variant in *GUCY2D*) showing macular atrophy. The color fundus photograph (**K**) showed atrophic macular mottling, and the fundus autofluorescence image (**L**) showed a small hyperautofluorescent center surrounded by a hypoautofluorescent ring with a hyperautofluorescent border. Spectral-domain OCT (**M**) revealed macular thinning with an absent central EZ and ELM and attenuated outer nuclear layer (BCVA in both eyes 20/400). **N–P,** A color fundus photograph (**N**), a fundus autofluorescence image (**O**), and an SD-OCT image (**P**) of the right eye of a 52-year-old patient (c.2513G>A; p.(Arg838His) *GUCY2D* variant) with marked atrophy of the central macula. Fundus photography shows central chorioretinal atrophy (**N**). This area corresponds to an absence of autofluorescence (**O**) and profound atrophy of the central retina on SD-OCT (**P**). **Q–T,** A color fundus photograph (**Q**), a fundus autofluorescence image (**R**), and SD-OCT scans (**S, T**) of a 46-year-old patient (c.2512C>T; p.(Arg838Cys) *GUCY2D* variant) with extensive macular, parapapillary, and peripheral atrophy. An absence of autofluorescence can be seen in a relatively large central area and around the optic disc, surrounded by a hyperautofluorescent border (**R**). Thinning of the retina around the optic disc can also be seen on SD-OCT (**S, T**). The BCVA of this eye was counting fingers in both eyes. BCVA = best-corrected visual acuity; CORD = cone–rod dystrophy; ELM = external limiting membrane; EZ = ellipsoid zone; SD-OCT = spectral-domain OCT.

Table 2. Imaging Findings in Patients with *GUCY2D*-Associated Cone–Rod Dystrophy and Leber Congenital Amaurosis at First Visit

	Cone–Rod Dystrophy	n (%)	Age (Yrs)
FAF	Increased foveal AF or hyper-AF	16/45 (36)	5.5–67.9
	Increased foveal AF or hyper-AF with hyper-AF borders	4/45 (9)	12.9–56.5
	Central granular AF with hyper-AF borders	13/45 (29)	33.2–65.4
	Central AF absence with hyper-AF borders	6/45 (13)	36.2–49.6
	Central AF absence without hyper-AF borders	4/45 (9)	36.2–49.6
	Other FAF pattern	2/45 (4)	35.7–54.2
	Structural Integrity on SD-OCT		
EZ	Intact	9/47 (19)	5.6–37.0
	Disrupted	9/47 (19)	12.5–68.0
	Absent	29/47 (62)	27.4–70.2
ELM	Intact	18/46 (39)	5.6–68.0
	Disrupted	4/46 (9)	12.8–37.0
	Absent	24/46 (52)	27.4–70.2
	Leber Congenital Amaurosis	**n (%)**	**Age (yrs)**
	Normal FAF pattern	1/5 (20)	15.5
	Increased foveal AF or hyper-AF	2/5 (40)	9.8–28.9
	Foveal hyper-AF with hyper-AF borders	1/5 (20)	10.3
	Hyper-AF ring only	1/5 (20)	28.1
	Structural Integrity on SD-OCT		
EZ/ELM	Intact	3/3 (100)	12.0–28.0

AF = autofluorescence; ELM = external limiting membrane; EZ = ellipsoid zone; FAF = fundus autofluorescence; SD-OCT = spectral-domain OCT.

The chorioretinal atrophy in advanced cases of *GUCY2D*-associated CORD can also resemble end-stage central areolar choroidal dystrophy associated with the *PRPH2* gene or geographic atrophy found in end-stage atrophic age-related macular degeneration.[24–26] The resemblance with age-related macular degeneration has also been described in other IRDs, but the absence of drusen and, in most cases, the early onset around the second decade of life of *GUCY2D*-associated CORD are helpful in differentiating the condition from age-related macular degeneration[26]; however, 1 patient displayed drusenoid, hyperautofluorescent dots on FAF and later developed atrophy (Fig 3D–H), which could complicate differentiation.

It is noteworthy that 3 patients who were screened for CORD at young ages because of known affected family members had isolated tritan color vision disturbances without other clear abnormalities or symptoms.[15] This could indicate that the S-cones, which are sensitive to blue light, may be affected first in *GUCY2D*-associated CORD and that tritan color vision defects may be the earliest measurable symptoms. This finding has not only been described earlier in young patients with *GUCY2D*-associated CORD but has also been found in CORD associated with pathologic variants in the *IRXB* gene cluster.[27,28] The early S-cone dysfunction may be due to the fact that these cones are more vulnerable to light-induced cell damage, which may be exacerbated by an underlying genetic condition.[29] Another explanation could be that the area around the foveal center, which contains the majority of S-cones, is affected first in some IRDs.

The c.2513G>A (p.(Arg838His)) and c.2512C>T (p.(Arg838Cys)) variants were, by far, the most common in patients with *GUCY2D*-associated CORD in the current cohort, similar to earlier studies, which described approximately 87% of *GUCY2D*-associated CORD cases to be associated with these variants.[10,30] A literature review of 132 patients with *GUCY2D*-associated CORD reported that the c.2513G>A (p.(Arg838His)) variant may be associated with a more severe phenotype than the c.2512C>T (p.(Arg838Cys)) variant, which was not the case in this cohort of 68 patients.[10] Considerable phenotypic variability was observed between subjects in this study, even within families carrying the same *GUCY2D* variant. For example, in the previously described large family with the c.2513G>A (p.(Arg838His) variant, 1 patient had a BCVA of 20/33 and another had a BCVA of 20/285, both at the age of 35 years. This high degree of interindividual variability, even within families, is well known in other autosomal dominant IRDs, such as those associated with the *BEST1* and *PRPH2* genes.[31,32] The large phenotypic variability in autosomal dominant diseases has been attributed to many factors, such as genetic modifiers, allelic variation, variable gene expression, and environmental factors.[33–36] Incomplete penetrance and variable expressivity have also been documented in other *GUCY2D*-associated CORD cohorts, but no clear underlying mechanism or combination of factors that explains this phenotypic

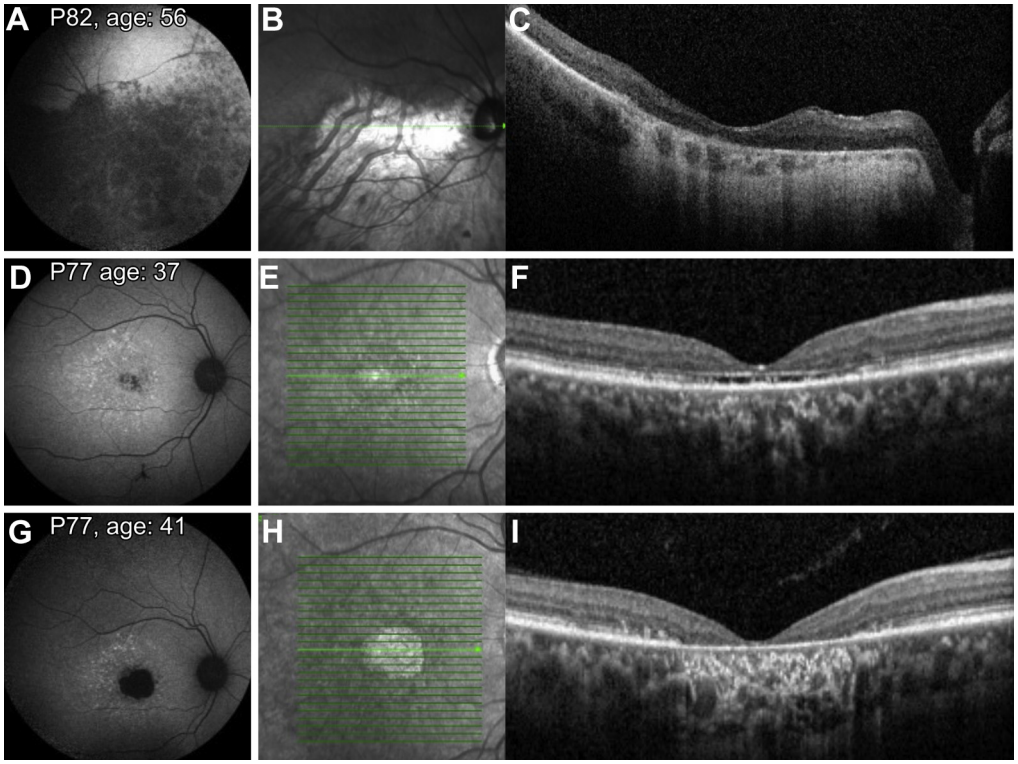

Figure 4. Atypical imaging findings in CORD associated with *GUCY2D*. **A–C,** A fundus autofluorescence image (**A**), a near-infrared image (**B**), and an SD-OCT scan (**C**) of a patient (c.2511_2512delinsCA; p.(Glu837_Arg838delinsAspSer) complex variant) with an atypical *GUCY2D*-associated CORD phenotype with extensive atrophic changes in the entire inferior pole. The visual acuity was 1.8 logMAR. **D,** Fundus autofluorescence image of a patient (c.2513G>A; p.(Arg838His) *GUCY2D* variant) with drusenoid hyperautofluorescent dots and an optical gap on SD-OCT (**F**). During follow-up, the patient developed macular atrophy (**G–I**). CORD = cone–rod dystrophy; logMAR = logarithm of the minimum angle of resolution; SD-OCT = spectral-domain OCT.

variability has been established yet.[13] We observed a high degree of symmetry in BCVA between the right and left eyes in patients with LCA as well as in patients with CORD, which would support the use of the fellow eye as an untreated control eye in future trials. Furthermore, our data suggested that there may be a relatively large window of opportunity for gene therapy in *GUCY2D*-associated LCA because the visual acuity and photoreceptor layers on the available imaging seemed to remain relatively stable during the follow-up. In patients with *GUCY2D*-associated CORD, severe visual impairment generally started to occur around the fourth decade of life, which suggests that the optimal window of opportunity for future treatments may lie within the first 3 to 4 decades of life; however, some patients with CORD above this age showed relatively intact photoreceptor layers and visual acuity, which would suggest that older individuals may also be eligible for future therapeutic intervention. The increasingly compromised integrity of the EZ and ELM layers, as well as a decrease in CRT, correlated significantly with a decrease in visual acuity, which has also been found previously for several other retinal dystrophies.[37,38] This may imply that these structural parameters may be suitable criteria for treatment candidate selection and may serve as (surrogate) end points in future therapeutic trials; however, prospective natural history studies may be necessary to validate and possibly further develop these end points by potentially also including the quantitative measurement of changes in these layers. The retrospective nature of this study is associated with certain inherent limitations, such as variability in the available data and in the intervals between visits. Especially for the patients with LCA, qualitative sufficient imaging and long-term follow-up were limited, and future studies with more long-term follow-up may be needed to better understand the spectrum and natural course of *GUCY2D*-associated LCA. Furthermore, similarly to earlier cohorts, only a few different variants were described for the patients with CORD in the current study, and these may not represent the entire phenotypic spectrum for *GUCY2D*-associated CORD.[10,30,39] Nonetheless, we have described the currently largest cohort of *GUCY2D*-associated retinal dystrophies and included longitudinal data, contrary to most of the earlier studies. Studies such as the current one are not only important to facilitate clinical counseling; they can also aid in choosing the optimal design for future therapeutic and prospective natural history studies.

Footnotes and Disclosures

Originally received: November 23, 2021.
Final revision: February 20, 2022.
Accepted: March 14, 2022.
Available online: March 18, 2022. Manuscript no. ORET-D-21-00663R1.

[1] Department of Ophthalmology, Amsterdam University Medical Centers, University of Amsterdam, Amsterdam, The Netherlands.

[2] Moorfields Eye Hospital National Health Service Foundation Trust, London, United Kingdom.

[3] Bartiméus Diagnostic Center for Complex Visual Disorders, Zeist, The Netherlands.

[4] Department of Clinical Genetics, Amsterdam University Medical Centers, University of Amsterdam, Amsterdam, The Netherlands.

[5] Department of Epidemiology and Data Science, Amsterdam University Medical Centers, Vrije Universiteit Amsterdam, Amsterdam, The Netherlands.

[6] Department of Ophthalmology, Ghent University Hospital, Ghent University, Ghent, Belgium.

[7] Center for Medical Genetics Ghent, Ghent University Hospital & Ghent University, Ghent, Belgium.

[8] Department of Ophthalmology, St James's University Hospital, Leeds, United Kingdom.

[9] Department of Ophthalmology, Erasmus Medical Center, Rotterdam, The Netherlands.

[10] Oxford Eye Hospital, John Radcliffe Hospital, Oxford University Hospitals National Health Service Foundation Trust, & Nuffield Laboratory of Ophthalmology, University of Oxford, Oxford, United Kingdom.

[11] Eye Unit, University Hospital Southampton, Southampton, United Kingdom.

[12] Department of Ophthalmology, University Medical Center Utrecht, Utrecht, The Netherlands.

[13] The Rotterdam Eye Hospital and the Rotterdam Ophthalmic Institute, Rotterdam, The Netherlands.

[14] Department of Ophthalmology, Radboud University Medical Center, Nijmegen, The Netherlands.

[15] The Netherlands Institute for Neuroscience (NIN-KNAW), Amsterdam, The Netherlands.

[16] Division of Ophthalmology and Center for Cellular and Molecular Therapeutics, Children's Hospital of Philadelphia, Philadelphia, Pennsylvania.

[17] UCL Institute of Ophthalmology, University College London, London, United Kingdom.

[18] Department of Ophthalmology, Leiden University Medical Center, Leiden, The Netherlands.

Disclosure(s):

All authors have completed and submitted the ICMJE disclosures form.

The authors have no proprietary or commercial interest in any materials discussed in this article.

Supported by the ODAS foundation (grant 2018-2 [C.J.F.B]) and the European Society of Retina Specialists (EURETINA Clinical Research Award 2019, grant 2019-1974 [L.C.H., C.J.F.B]).

The collection of data in the participating centers was partially supported by the Ghent University Special Research Fund (BOF15/GOA/011 to E.D.B. and BOF20/GOA/023 to E.D.B. and B.P.L.) and by the Ghent University Hospital Innovation Fund (NucleUZ to E.D.B.). E.D.B. (1802220N) and B.P.L. (1803821N) are Senior Clinical Investigators of the Fonds voor Wetenschappelijk Onderzoek. Furthermore, this work has also been supported by grants from the National Institute for Health Research Biomedical Research Centre at Moorfields Eye Hospital NHS Foundation Trust and UCL Institute of Ophthalmology, Moorfields Eye Charity, and Retina UK. The Oxford EYE Hospital was supported by the Oxfordshire and South Midlands Clinical Research Network and the UK Inherited Retinal Dystrophy Consortium Project (Retina UK, GR586). The views expressed are those of the authors and not necessarily those of the NHS, the NIHR, or the Department of Health. Saoud Al-Khuzaei is supported by a scholarship from the Qatar National Research Fund (GSRA6-1-0329-19010). The RD5000 consortium was supported by Uitzicht (grant 2015-30 financed by ODAS, Oogfonds, Retinafonds and Bartiméus Sonneheerdt).

This study was performed as part of a collaboration within the Dutch RD5000 network for rare retinal dystrophies, and the European Reference Network for Rare Eye Diseases (ERN-EYE). E.D.B., C.C.W.K., L.I.v.d.B., C.B.H, B.P.L., A.A.B. & C.J.F.B. are members of ERN-EYE, which is co-funded by the Health Program of the European Union under the Framework Partnership Agreement No 739534 'ERN-EYE'. The sponsors, funding or collaborating organizations had no role in the design or conduct of this research.

Presented at the annual meeting of the Netherlands Ophthalmological Society, virtual conference, March 24 - March 26, 2021; the annual meeting of the Association for Research in Vision and Ophthalmology, virtual conference, May 1 - May 7, 2021; and the annual meeting of the European Society of Retina Specialists, virtual conference, September 9 - September 12, 2021.

HUMAN SUBJECTS: Human subjects were included in this study. This study was approved by the ethics committee of the Erasmus Medical Center and adhered to the tenets of the Declaration of Helsinki. Informed consent was obtained from patients or their legal guardians. For patients of the University Hospital Ghent the need for informed consent was waived by the local ethics committee since only pseudonymized data was used.

No animal subjects were used in this study.

Author Contributions:

Conception and design: Hahn, van Schooneveld, Wesseling, Boon

Analysis and interpretation: Hahn, Georgiou, Almushattat, van Schooneveld, Florijn, Lissenberg-Witte, Boon

Data collection: Hahn, Almushattat, van Schooneveld, de Carvalho, Wesseling, ten Brink, Strubbe, van Cauwenbergh, de Zaeytijd, Walraedt, de Baere, Mukherjee, McKibbin, Meester-Smoor, Thiadens, Al-Khuzaei, Akyol, Lotery, van Genderen, Ossewaarde-van Norel, van den Born, Hoyng, Klaver, Downes, Bergen, Leroy, Michaelides, Boon

Obtained funding: N/A

Overall responsibility: Hahn, Georgiou, Almushattat, van Schooneveld, de Carvalho, Wesseling, ten Brink, Florijn, Lissenberg-Witte, Strubbe, van Cauwenbergh, de Zaeytijd, Walraedt, de Baere, Mukherjee, McKibbin, Meester-Smoor, Thiadens, Al-Khuzaei, Akyol, Lotery, van Genderen, Ossewaarde-van Norel, van den Born, Hoyng, Klaver, Downes, Bergen, Leroy, Michaelides, Boon

Abbreviations and Acronyms:
BCVA = best-corrected visual acuity; **CORD** = cone–rod dystrophy; **CRT** = central retinal thickness; **ELM** = external limiting membrane; **ERG** = electroretinography; **EZ** = ellipsoid zone; **FAF** = fundus autofluorescence; **IQR** = interquartile range; **IRD** = inherited retinal dystrophy; **LCA** = Leber congenital amaurosis; **logMAR** = logarithm of the minimum angle of resolution; **RPE** = retinal pigment epithelium; **SD-OCT** = spectral-domain OCT

Keywords:
Cone–rod dystrophy, *GUCY2D*, Inherited retinal dystrophies, Leber congenital amaurosis, Phenotype.

Correspondence:
Camiel J.F. Boon, MD, PhD, Department of Ophthalmology, Amsterdam University Medical Centers, PO Box 22660, 1100 DD Amsterdam, The Netherlands. E-mail: Camiel.boon@amsterdamumc.nl.

References

1. Ellingford JM, Barton S, Bhaskar S, et al. Molecular findings from 537 individuals with inherited retinal disease. *J Med Genet*. 2016;53:761−767.
2. Kumaran N, Moore AT, Weleber RG, Michaelides M. Leber congenital amaurosis/early-onset severe retinal dystrophy: clinical features, molecular genetics and therapeutic interventions. *Br J Ophthalmol*. 2017;101:1147−1154.
3. Gill JS, Georgiou M, Kalitzeos A, et al. Progressive cone and cone-rod dystrophies: clinical features, molecular genetics and prospects for therapy. *Br J Ophthalmol*. 2019;103:711−720.
4. Bouzia Z, Georgiou M, Hull S, et al. GUCY2D-associated Leber congenital amaurosis: a retrospective natural history study in preparation for trials of novel therapies. *Am J Ophthalmol*. 2020;210:59−70.
5. Downes SM, Payne AM, Kelsell RE, et al. Autosomal dominant cone-rod dystrophy with mutations in the guanylate cyclase 2D gene encoding retinal guanylate cyclase-1. *Arch Ophthalmol*. 2001;119:1667−1673.
6. Smith M, Whittock N, Searle A, et al. Phenotype of autosomal dominant cone-rod dystrophy due to the R838C mutation of the GUCY2D gene encoding retinal guanylate cyclase-1. *Eye (Lond)*. 2007;21:1220−1225.
7. Wimberg H, Lev D, Yosovich K, et al. Photoreceptor guanylate cyclase (GUCY2D) mutations cause retinal dystrophies by severe malfunction of Ca(2+)-dependent cyclic GMP synthesis. *Front Mol Neurosci*. 2018;11:348.
8. Boye SL, Peterson JJ, Choudhury S, et al. Gene therapy fully restores vision to the all-cone Nrl(-/-) Gucy2e(-/-) mouse model of Leber congenital amaurosis-1. *Hum Gene Ther*. 2015;26:575−592.
9. Jacobson SG, Cideciyan AV, Ho AC, et al. Safety and improved efficacy signals following gene therapy in childhood blindness caused by GUCY2D mutations. *iScience*. 2021;24:102409.
10. Sun Z, Wu S, Zhu T, et al. Variants at codon 838 in the GUCY2D gene result in different phenotypes of cone rod dystrophy. *Ophthalmic Genet*. 2020;41:548−555.
11. McCullough KT, Boye SL, Fajardo D, et al. Somatic gene editing of GUCY2D by AAV-CRISPR/Cas9 alters retinal structure and function in mouse and macaque. *Hum Gene Ther*. 2019;30:571−589.
12. van Huet RAC, Oomen CJ, Plomp AS, et al. The RD5000 database: facilitating clinical, genetic, and therapeutic studies on inherited retinal diseases. *Invest Ophthalmol Vis Sci*. 2014;55:7355−7360.
13. Udar N, Yelchits S, Chalukya M, et al. Identification of GUCY2D gene mutations in CORD5 families and evidence of incomplete penetrance. *Hum Mutat*. 2003;21:170−171.
14. Mukherjee R, Robson AG, Holder GE, et al. A detailed phenotypic description of autosomal dominant cone dystrophy due to a de novo mutation in the GUCY2D gene. *Eye (Lond)*. 2014;28:481−487.
15. Went LN, van Schooneveld MJ, Oosterhuis JA. Late onset dominant cone dystrophy with early blue cone involvement. *J Med Genet*. 1992;29:295−298.
16. The RFoundationR. A language and environment for statistical computing. https://www.R-project.org/. Accessed January 12, 2020.
17. Putter H, Fiocco M, Geskus RB. Tutorial in biostatistics: competing risks and multi-state models. *Stat Med*. 2007;26:2389−2430.
18. Ying GS, Maguire MG, Glynn R, Rosner B. Tutorial on biostatistics: statistical analysis for correlated binary eye data. *Ophthalmic Epidemiol*. 2018;25:1−12.
19. Csaky KG, Richman EA, Ferris III FL. Report from the NEI/FDA ophthalmic clinical trial design and endpoints symposium. *Invest Ophthalmol Vis Sci*. 2008;49:479−489.
20. Liu X, Fujinami K, Kuniyoshi K, et al. Clinical and genetic characteristics of 15 affected patients from 12 Japanese families with GUCY2D-associated retinal disorder. *Transl Vis Sci Technol*. 2020;9:2.
21. Jacobson SG, Cideciyan AV, Sumaroka A, et al. Defining outcomes for clinical trials of Leber congenital amaurosis caused by GUCY2D mutations. *Am J Ophthalmol*. 2017;177:44−57.
22. Jacobson SG, Cideciyan AV, Sumaroka A, et al. Leber congenital amaurosis due to GUCY2D mutations: longitudinal analysis of retinal structure and visual function. *Int J Mol Sci*. 2021;22(4):2031.
23. van Dijk EHC, Boon CJF. Serous business: delineating the broad spectrum of diseases with subretinal fluid in the macula. Prog Retin Eye Res. 2021(84):100955.
24. Boon CJ, Klevering BJ, Cremers FP, et al. Central areolar choroidal dystrophy. *Ophthalmology*. 2009;116:771−782, 782.e771.
25. Smailhodzic D, Fleckenstein M, Theelen T, et al. Central areolar choroidal dystrophy (CACD) and age-related macular degeneration (AMD): differentiating characteristics in multimodal imaging. *Invest Ophthalmol Vis Sci*. 2011;52:8908−8918.
26. Saksens NTM, Fleckenstein M, Schmitz-Valckenberg S, et al. Macular dystrophies mimicking age-related macular degeneration. *Prog Retin Eye Res*. 2014;39:23−57.
27. Gregory-Evans K, Kelsell RE, Gregory-Evans CY, et al. Autosomal dominant cone−rod retinal dystrophy (CORD6) from heterozygous mutation of GUCY2D, which encodes retinal guanylate cyclase. *Ophthalmology*. 2000;107:55−61.
28. Kohl S, Llavona P, Sauer A, et al. A duplication on chromosome 16q12 affecting the IRXB gene cluster is associated with autosomal dominant cone dystrophy with early tritanopic color vision defect. *Hum Mol Genet*. 2021;30:1218−1229.
29. Haverkamp S, Wässle H, Duebel J, et al. The primordial, blue-cone color system of the mouse retina. *J Neurosci*. 2005;25:5438−5445.
30. Yi Z, Sun W, Xiao X, et al. Novel variants in GUCY2D causing retinopathy and the genotype-phenotype correlation. *Exp Eye Res*. 2021;208:108637.
31. Boon CJF, Klevering BJ, Leroy BP, et al. The spectrum of ocular phenotypes caused by mutations in the BEST1 gene. *Prog Retin Eye Res*. 2009;28:187−205.
32. Boon CJ, den Hollander AI, Hoyng CB, et al. The spectrum of retinal dystrophies caused by mutations in the peripherin/RDS gene. *Prog Retin Eye Res*. 2008;27:213−235.
33. Green DJ, Sallah SR, Ellingford JM, et al. Variability in gene expression is associated with incomplete penetrance in inherited eye disorders. *Genes (Basel)*. 2020;11:179.
34. Cooper DN, Krawczak M, Polychronakos C, et al. Where genotype is not predictive of phenotype: towards an

understanding of the molecular basis of reduced penetrance in human inherited disease. *Hum Genet*. 2013;132:1077–1130.
35. Scheetz TE, Kim KY, Swiderski RE, et al. Regulation of gene expression in the mammalian eye and its relevance to eye disease. *Proc Natl Acad Sci U S A*. 2006;103:14429–14434.
36. Gui B, Slone J, Huang T. Perspective: is random monoallelic expression a contributor to phenotypic variability of autosomal dominant disorders? *Front Genet*. 2017;8:191.
37. Nguyen XT, Talib M, van Cauwenbergh C, et al. Clinical characteristics and natural history of RHO-associated retinitis pigmentosa: a long-term follow-up study. *Retina*. 2021;41:213–223.
38. Tee JJL, Yang Y, Kalitzeos A, et al. Natural history study of retinal structure, progression, and symmetry using ellipzoid zone metrics in RPGR-associated retinopathy. *Am J Ophthalmol*. 2019;198:111–123.
39. Kitiratschky VB, Wilke R, Renner AB, et al. Mutation analysis identifies GUCY2D as the major gene responsible for autosomal dominant progressive cone degeneration. *Invest Ophthalmol Vis Sci*. 2008;49:5015–5023.

Pictures & Perspectives

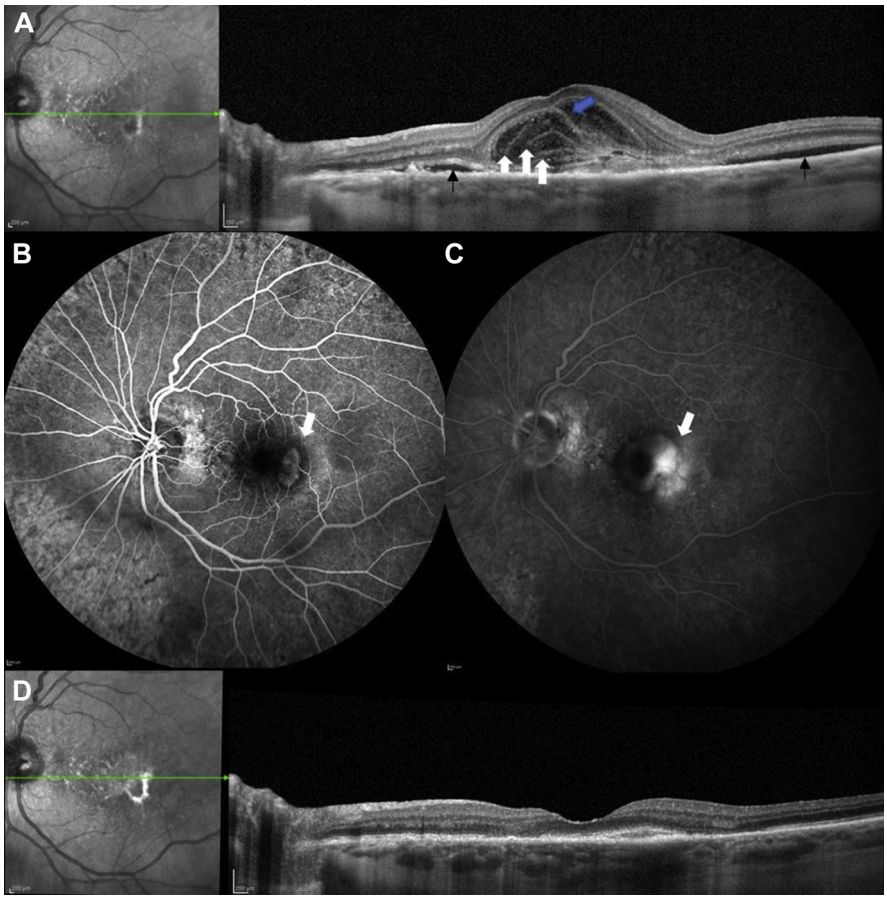

Bacillary Layer Detachment in Age-Related Macular Degeneration

An 81-year-old woman presented with a dark spot in her left eye for 4 days with a visual decrease from 20/25 to 20/80. **A**, OCT at presentation demonstrated subretinal fluid (black arrows), bacillary layer detachment (blue arrow), and splitting of photoreceptor layers resulting in additional hyperreflective layers (white arrows). **B,** Early and (**C**) late-phase fluorescein angiography showing leakage from macular neovascularization (white arrows) temporal to the fovea, consistent with exudative age-related macular degeneration. **D**, OCT after treatment with 3 intravitreal bevacizumab 1.25 mg per 0.05 mL injections demonstrating resolution of subretinal fluid and bacillary layer detachment with improvement in vision to 20/30. (Magnified version of Fig **A-D** is available online at www.ophthalmololgyretina.org).

Melis Kabaalioglu Guner, MD
Matthew R. Starr, MD

Department of Ophthalmology, Mayo Clinic, Rochester, Minnesota